

## Relationship between Neural, Vascular, and BOLD Signals in Isoflurane-Anesthetized Rat Somatosensory Cortex

Kazuto Masamoto, Tae Kim, Mitsuhiro Fukuda,  
Ping Wang and Seong-Gi Kim

Departments of Radiology and Neurobiology, University of  
Pittsburgh, Pittsburgh, Pennsylvania, USA

**Functional magnetic resonance imaging (fMRI) in anesthetized rodents has been commonly performed with  $\alpha$ -chloralose, which can be used only for terminal experiments. To develop a survival fMRI protocol, an isoflurane (ISO) -anesthetized rat model was systematically evaluated by simultaneous measurements of field potential (FP) and cerebral blood flow (CBF) in the somatosensory cortex. A conventional forepaw stimulation paradigm with 0.3 ms pulse width, 1.2 mA current, and 3 Hz frequency induced 54% less evoked FP and 84% less CBF response under ISO than  $\alpha$ -chloralose. To improve stimulation-induced responses under ISO, 10-pulse stimulations were performed with variations of width, current, and frequency. For widths of 0.1–5.0 ms and currents of 0.4–2.0 mA, evoked FP and CBF increased similarly and reached a plateau. The evoked FP increased monotonically for intervals from 50 to 500 ms, but the CBF peaked at an interval of 83 ms (~12 Hz frequency). These data suggest that different anesthetics profoundly affect FP and CBF responses in different ways, which requires optimizing stimulation parameters for each anesthetic. With the refined stimulation parameters, fMRI consistently detected a well-localized activation focus at the primary somatosensory cortex in ISO-anesthetized rats. Thus, the ISO-anesthetized rat model can be used for cerebrovascular activation studies, allowing repeated noninvasive survival experiments.**

**Keywords:** anesthesia, frequency tuning, laser Doppler flowmetry, local field potential, longitudinal fMRI, neurovascular coupling

### Introduction

Hemodynamic-based functional magnetic resonance imaging (fMRI), which relies on changes in hemodynamic signals induced by neural activation, can be used to noninvasively measure changes in brain functions in the same subject over time. Most rodent fMRI studies have been performed with  $\alpha$ -chloralose (Hyder and others 1994; Gyngell and others 1996; Mandeville and others 1998; van Bruggen and others 1998; Silva and others 1999) because it 1) preserves metabolic coupling for somatosensory stimulation (Ueki and others 1992), 2) provides good stability of baseline blood flow (Lindauer and others 1993), and 3) preserves cerebrovascular reactivity (Bonvento and others 1994). However,  $\alpha$ -chloralose can be used only for “terminal” experiments (Silverman and Muir 1993), which hampers the utility of rodent fMRI to investigate long-term changes in brain function.

In order to perform “survival” experiments, inhalant anesthetics (e.g., isoflurane [ISO]) should be considered. ISO has been used successfully in repeated survival fMRI studies with other species (e.g., cats and monkeys) (Logothetis and others 1999; Kim and others 2000; Duong and others 2001), and it is widely used for physiological studies (Lukasik and Gillies 2003).

Recently, a detectable fMRI signal was reported in an ISO-anesthetized rat when unusually strong forepaw electrical stimulation (>6 mA current) was applied (Liu and others 2004). However, this strong stimulation induced a significant change in systemic blood pressure, indicating that the stimulation is painful and evokes global hemodynamic changes; thus, it is not suitable for somatosensory stimulation. Therefore, stimulation paradigm should have robust fMRI responses without any influence on systemic blood pressure. Because anesthetics work via different mechanisms and may therefore affect neural activity and/or vascular reactivity differently, it is necessary to measure neural and vascular responses under ISO to optimize stimulation parameters for this particular anesthetic.

To refine stimulation parameters under ISO, we measured local field potential (FP) and cerebral blood flow (CBF) in the rat somatosensory cortex during forepaw stimulation. To compare responses under  $\alpha$ -chloralose and ISO in the same animal, we used standard stimulation parameters with 0.3 ms pulse width, 1.2 mA current, and 3 Hz frequency (Silva and others 1999). To evaluate the neural and vascular responses under ISO, we varied stimulation parameters (pulse width, current, and onset-to-onset intervals). Finally, we performed blood oxygenation level-dependent (BOLD) fMRI of ISO-anesthetized rats with the refined stimulation parameters to determine whether BOLD signals were detected.

### Materials and Methods

#### General Preparation

A total of 17 male Sprague-Dawley rats (340–440 g; Charles River Laboratories, Wilmington, MA) were used with experimental protocols approved by the University of Pittsburgh Institutional Animal Care and Use Committee in accordance with the standards for humane animal care and use as set by the Animal Welfare Act and the National Institutes of Health Guide for the Care and Use of Laboratory Animals. The animals were initially anesthetized with ISO (5% for induction and 1.5–2% during endotracheal intubation and surgery) via a calibrated vaporizer with a mixture of O<sub>2</sub> (35–50%) and N<sub>2</sub>O (50–65%). Endotracheal intubation was performed for mechanical ventilation, a catheter was placed into the femoral vein for later infusion of  $\alpha$ -chloralose, and the femoral artery was catheterized for arterial blood pressure monitoring and blood gas sampling. For FP and CBF measurements, the animals were placed in a stereotaxic frame (Narishige International USA, Inc., East Meadow, NY), and an area (5 mm × 7 mm) on the left skull centered 3.5 mm lateral and 0.5 mm rostral from the “bregma” (Hall and Lindholm 1974) was thinned with a drill (Lindauer and others 1993).

After the surgical preparation was complete, the inspired gas was converted to a mixture of air and O<sub>2</sub> (30–35% total O<sub>2</sub>), and the concentration of end-tidal ISO was adjusted to ~1 minimum alveolar concentration (MAC), ISO = 1.3 ± 0.1% in rats (Eger and others 1965; Antognini and others 1999). End-tidal CO<sub>2</sub> and ISO levels were monitored with a capnometer (Capnomac Ultima™, Datex-Ohmeda, Inc., Madison, WI). The physiological conditions (i.e., end-tidal gas

concentrations, arterial blood pressure, and electrocardiogram) were recorded with polygraph data acquisition software (AcqKnowledge, BIOPAC systems, Inc., Goleta, CA). Minute ventilation volume (150–220 mL/min) and respiratory rate (50–60 breaths/min) were adjusted with the ventilator (Topo™, Kent Scientific Corp., Torrington, CT) as needed. The blood gas was maintained within physiological limits. Rectal temperature was maintained at  $37.0 \pm 0.2$  °C with a constant current temperature feedback control module (40-90-8C, FHC, Inc., Bowdoinham, ME).

For the stimulation, 2 needle electrodes (30G 1/2") were inserted under the skin between digits 2 and 4 of the right forepaw (Silva and others 1999). Electrical pulse stimulation was given with a constant current bipolar stimulation isolator (A365D, World Precision Instruments, Inc., Sarasota, FL) triggered by a pulse generator (Master 8, AMPI, Israel). The parameters of the electrical stimulation were adjusted for each experiment as described below.

### Experimental Design

Three different studies were performed: "α-chloralose versus ISO" ( $N=5$  animals), "Neurovascular responses under ISO" ( $N=7$ ), and "BOLD fMRI under ISO" ( $N=5$ ). In both the α-chloralose versus ISO and neurovascular responses under ISO studies, FP and CBF were simultaneously measured with a tungsten microelectrode and laser Doppler flowmetry (LDF), respectively, at the activation focus predetermined by intrinsic optical imaging (see Fig. 1A,B). The BOLD fMRI under ISO study was

performed on a 9.4-T magnetic resonance imaging (MRI) system. All data were reported as mean  $\pm$  standard deviation (SD), and statistical analysis was performed with paired Student's *t*-test ( $P < 0.05$ ).

The α-chloralose versus ISO experiment was performed in the same animal with the same stimulation parameters for both α-chloralose and ISO. The 10 rectangular pulses (see Fig. 1C) with 0.3 ms width, 1.2 mA current, and 333-ms interval (i.e., 3 Hz for 3-s duration) were applied as previously optimized under α-chloralose (Silva and others 1999). Twenty stimulation runs were repeated with an interrun time of 40 s. Baseline FP activity and CBF level (without stimulation) were also recorded for ~3 min before and after whole stimulation runs. After completion of all recordings under ISO (1 MAC), α-chloralose (45 mg/kg, intravenous [i.v.]) was induced, and ISO was discontinued. The subsequent anesthetic level was maintained by continuous injection of α-chloralose (45 mg/kg/h, i.v.). Based on our preliminary studies, the amplitude of baseline FP activity under ISO (1 MAC) was similar to that under α-chloralose (45 mg/kg/h). The adequate anesthetic level was assessed by foot pinch as needed. Approximately 70 min after the initial induction of α-chloralose, the recording was performed with exactly the same protocol used for the ISO study. Because α-chloralose has a longer lasting effect (6–10 h; Lees 1972; Silverman and Muir 1993) than ISO (~5 min, Hayton and others 1999), the recordings under α-chloralose followed ISO experiments. Each experiment was performed within ~1 h to minimize time-dependent variations (Austin and others 2005).

The neurovascular responses under ISO experiments were performed with varying stimulation parameters (pulse width, current, and onset-to-onset interval) under ISO (1 MAC). The stimulation parameters (10 pulses) were 1) 9 different widths (0.1–5.0 ms) with fixed current (1.0 mA) and interval (125 ms), 2) 10 different currents (0.2–2.0 mA) with fixed width (1.0 ms) and interval (125 ms), and 3) 9 different intervals (50–500 ms) with fixed width (1.0 ms) and current (1.0 mA). It should be noted that the interval (e.g., 50–500 ms) is an inverse of the stimulation frequency (e.g., 20–2 Hz). These ranges of parameter variations are commonly used for electrical stimulation in rat somatosensory cortex studies. The experimental order of the 3 variation groups (1, 2, and 3) was randomized in each of 5 animals, and the other 2 animals were used only for the interval variations. In each group (1, 2, and 3), the target parameter was sequentially varied from the lowest value to the highest (ascending order) or from the highest value to the lowest (descending order). Six to 11 runs were repeated for each parameter with an interrun time of 40 s.

The BOLD fMRI under ISO study was performed on a 9.4-T MRI system under ISO (1 MAC) with the stimulation parameters refined in the aforementioned neurovascular responses study. Because BOLD is directly related to venous oxygenation level, it is possible that the stimulation parameters determined by CBF measurements with LDF may not induce detectably strong BOLD responses. To validate BOLD responses evoked by the refined parameters, the 10-pulse stimulation with fixed width and current was applied with various stimulation frequencies (3, 6, 12, and 20 Hz). The current was slightly adjusted to obtain high BOLD response without influencing systemic blood pressure in the animals (i.e., 1.0 ms width and 1.4–1.7 mA current). Each fMRI run was repeated 10–15 times with an interrun time of 1 min.

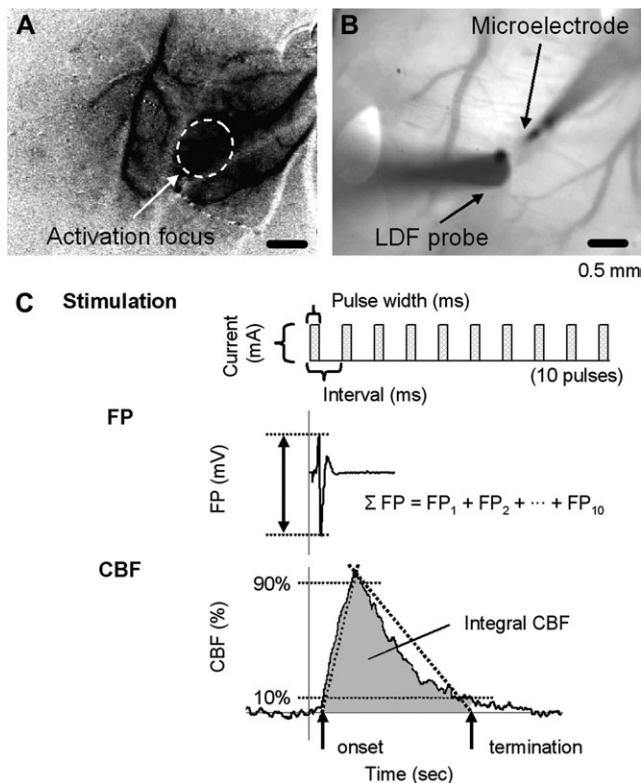


**Figure 1.** (A) Optical imaging map. The darkened area shows the decrease in light reflectance (620-nm wavelength) from prestimulation level in response to electrical forepaw stimulation. The white circle with a dashed line represents activation focus (~1-mm diameter). The localized activation focus was consistently observed in all animals. The stimulation-induced reflectance change ( $\Delta R/R$ ) in the activation focus was ~0.2%. (B) Probe locations for recording of evoked FP and CBF at the activation focus. The distance between the microelectrode insertion and LDF probe was ~0.5 mm. (C) Definition of stimulation parameters and calculation of evoked FP and CBF. Ten rectangular pulses of electrical stimulation were induced with varying 1) pulse width, 2) current, and 3) onset-to-onset interval. The amplitude of the evoked FP was measured from minimal peak to maximal peak. The summation of evoked FP ( $\Sigma FP$ ) was then calculated to sum all amplitudes of 10 consecutive evoked FPs ( $FP_1 + FP_2 + \dots + FP_{10}$ ). The evoked CBF (integral CBF) was calculated to integrate the area of mean CBF response curve bounded from the time-to-onset to the time-to-termination of mean CBF curves (See text in detail).

### FP and CBF Measurements

#### Data Acquisition

To determine where to place the microelectrode for FP recording and the LDF probe for CBF measurement, we mapped the activation focus in the somatosensory cortex with optical imaging of intrinsic signals using a custom-made system (Moon and others 2004). The intrinsic signal images ( $640 \times 480$  pixels and  $4.9 \times 3.7$  mm<sup>2</sup> field of view [FOV]) were obtained with  $620 \pm 10$  nm wavelength, which is weighted by deoxyhemoglobin, at a rate of 30 frames/s. Temporal averaging of 15 consecutive frames and spatial binning of  $2 \times 2$  pixels were performed, resulting in a temporal resolution of 0.5 s and a matrix size of  $320 \times 240$ . Twenty runs were repeated and then averaged; each 6-s-long stimulation run was a 10-pulse stimulation with 1.0 ms width, 1.5 mA current, and 333-ms interval. The optical imaging map was calculated by the relative change in reflectance  $\Delta R/R$ , where  $\Delta R$  is the subtracted image intensity between an average of 2 prestimulation images ( $R$ ) and an

average of 4 activation images acquired 0.5–2.5 s after the onset of stimulation. The activation focus was determined around the largest decrease in reflectance  $\Delta R/R$  in the map (Narayan and others 1994; Nemoto and others 2004).

Based on this optical imaging map (Fig. 1A), a tungsten microelectrode ( $<1\text{ M}\Omega$ , a  $\sim 3\text{-}\mu\text{m}$  tip and a 0.2-mm shank diameter; FHC, Inc., Bowdoinham, ME) was inserted at the activation focus 0.5–0.6 mm below the cortical surface, where the largest evoked FP is observed (Nielsen and Lauritzen 2001). FP signals were acquired at a 1-kHz sampling rate using the BIOPAC system without filtering after amplifying 1000 times with the aid of Neural Data Acquisition software (Plexon, Inc., Dallas, TX). The reference electrode was positioned on the scalp. CBF signal was acquired via LDF (PeriFlux 4001Master, Perimed, Sweden) with a time constant of 0.03 s. The light source for the LDF was a 780-nm diode laser with a maximum accessible emission of 1 mW. A needle-type laser Doppler probe (0.45-mm tip diameter, 0.15-mm probe separation; Probe 411, Perimed, Sweden) was placed on the surface of the thinned skull at  $\sim 0.5\text{ mm}$  from the tungsten microelectrode (see Fig. 1B). To detect the signals mostly from the parenchymal tissue level, the probe was placed based on the visible cortical vascular networks, the baseline LDF value, and backscattered light level (Dirnagl and others 1989). The LDF generally sampled the movement of red blood cells in the vessels up to a depth of  $\sim 1\text{ mm}$  in the cortex (Arbit and DiResta 1996). Both FP and CBF data were simultaneously recorded on a PC with BIOPAC data acquisition software (AcqKnowledge, BIOPAC systems, Inc., Goleta, CA) at a sampling rate of 1 kHz.

#### Data Processing

To compare baseline conditions under  $\alpha$ -chloralose and ISO, baseline FP and CBF (without stimulation) were measured. Baseline FP activity was determined as the recorded voltage beyond threshold, which was set as mean  $\pm 2\text{ SD}$  of the system noise level. The noise level was determined at the end of the experiment by recording “activity” under the exact experimental conditions, except that the animal had been euthanized by i.v. injection of KCl. The recording was performed approximately 10 min after the injection of KCl. Magnitudes of positive and negative voltages beyond the threshold were summed during the recording period and normalized by the recording time (i.e., Base FP [mV]). Baseline CBF level was measured by averaging the LDF value across the recording period (i.e., Base CBF [a.u.]). It should be noted that the LDF value represents a relative perfusion rate (Stern and others 1977; Bonner and Nossal 1981). In our study, the LDF probe placement was fixed in the same position between the 2 anesthetic conditions, and the physiological parameters (systemic arterial blood pressure and blood gas) were maintained. Thus, the observed change in baseline LDF value mostly reflects the relative change in CBF level due to the anesthetics. The frequency composition of the baseline FP and CBF was analyzed with fast Fourier transform.

All runs with the same stimulation parameters were averaged, which resulted in one averaged FP data and one averaged CBF data at each condition in each animal. Quantitative analyses of FP and CBF data follow: 1) The amplitude of the evoked FP was calculated as the difference between the positive peak and the negative peak (see Fig. 1C). The sum of the evoked FP ( $\sum\text{FP}$ ) was then calculated as the sum of the amplitudes of all 10 evoked FPs ( $\text{FP}_1 + \text{FP}_2 + \dots + \text{FP}_{10}$ ). 2) The averaged CBF time course data was reduced to a temporal resolution of 0.2 s to improve signal-to-noise ratio and then normalized by the mean level of 4-s prestimulation data. Then, peak CBF response and time-to-peak were calculated. To incorporate both peak intensity and duration of CBF response, integral CBF was calculated as the area under the mean CBF curve from time-to-onset to time-to-termination (see Fig. 1C). The time-to-onset was determined as the intercept of the upward line passing through 2 points (10% and 90% of the CBF peak response before the peak) at the prestimulus baseline. Similarly, the time-to-termination was calculated as the intercept of the downward line passing through 2 points (90% and 10% of the CBF peak response after the peak) at the poststimulus baseline.

The  $\sum\text{FP}$  and integral CBF values were normalized by the values obtained at the common stimulus (1.0 ms, 1.0 mA, and 125 ms) in each experimental group in each animal to allow the comparison of their parameter dependence across different stimulations and across animals.

## BOLD fMRI

### Data Acquisition

BOLD fMRI was performed on a 9.4-T magnet interfaced to a Unity Inova console (Varian, Palo Alto, CA). The gradient coil was an actively shielded gradient set (12-cm inner diameter) with a strength of 40 G/cm and a rise time of 0.13 ms (Magnex, Abington, UK). The animal was secured in a home-built stereotaxic frame. A surface coil (2.3-cm diameter) was positioned on top of the rat’s head for imaging. The magnetic field was manually shimmed on a slab twice the thickness of the imaging slice. A single 2-mm-thick coronal slice covering the primary somatosensory cortex was selected. All images were acquired using an echo planar imaging sequence with gradient echo time of 20 ms, repetition time of 500 ms, data matrix of  $64 \times 32$  (readout direction  $\times$  phase-encoding direction), and FOV of  $30 \times 15\text{ mm}$  (right-left hemisphere  $\times$  dorsal-ventral directions). The power of the radio frequency pulse was adjusted to maximize the signals at the primary somatosensory cortex. For each fMRI run, a total of 50 images were acquired, including 10 prestimulus control images.

### Data Processing

Repeated fMRI runs were averaged. Then, the BOLD functional map was calculated using *F*-value analysis with the baseline period (5-s prestimulation) compared with the BOLD response period (2.0–3.5 s after the stimulation onset), which included the peaks of BOLD response observed for all 10-pulse stimulation. The region of interest (ROI) for the contralateral forepaw somatosensory cortex, consisting of  $3 \times 4$  pixels with 2 mm thickness, was selected according to a published stereotaxic atlas (Paxinos and Watson 1986). From the pixels within the ROI, the mean BOLD time course data were calculated and normalized by the baseline level (mean of 5-s prestimulation).

## Results

### Physiological Parameters

In the  $\alpha$ -chloralose versus ISO study group, we monitored physiological conditions of all animals ( $N = 5$ ) under ISO (mean arterial blood pressure [MABP] =  $88 \pm 5\text{ mm Hg}$ , pH =  $7.48 \pm 0.04$ , PaCO<sub>2</sub> =  $33 \pm 4\text{ mm Hg}$ , and PaO<sub>2</sub> =  $124 \pm 8\text{ mm Hg}$ ) and  $\alpha$ -chloralose (MABP =  $94 \pm 10\text{ mm Hg}$ , pH =  $7.46 \pm 0.01$ , PaCO<sub>2</sub> =  $37 \pm 1\text{ mm Hg}$ , and PaO<sub>2</sub> =  $109 \pm 5\text{ mm Hg}$ ); there were no significant differences. In the neurovascular responses under ISO group ( $N = 7$ ), the physiological conditions were MABP =  $96 \pm 10\text{ mm Hg}$ , pH =  $7.48 \pm 0.01$ , PaCO<sub>2</sub> =  $36 \pm 1\text{ mm Hg}$ , and PaO<sub>2</sub> =  $101 \pm 6\text{ mm Hg}$ . For the “fMRI group” ( $N = 5$ ), the physiological conditions were MABP =  $99 \pm 4\text{ mm Hg}$ , pH =  $7.46 \pm 0.03$ , PaCO<sub>2</sub> =  $36 \pm 3\text{ mm Hg}$ , and PaO<sub>2</sub> =  $120 \pm 12\text{ mm Hg}$ . In all experiments, no change in MABP was observed during stimulation.

### $\alpha$ -Chloralose versus ISO

The pattern of “baseline” FP activity was dependent on the anesthetics used (Fig. 2). Under 1 MAC ISO, spontaneous activities were sparse, but the burst signals had a high intensity. The power spectrum showed that frequency composition of 30–80 Hz is higher under ISO than  $\alpha$ -chloralose. The summed power of a 1- to 500-Hz frequency range under  $\alpha$ -chloralose was  $11 \pm 22\%$  ( $N = 5$ ) less than that of ISO. Note that the mean amplitude of the system noise level was  $0.011 \pm 0.006\text{ mV}$  ( $N = 5$ ), and its power spectrum was mostly flat, except for small peaks of electrical noise at 60 Hz (data not shown). The fluctuation levels (1 SD of mean) of baseline CBF were  $7.5 \pm 1.6\%$  and  $7.1 \pm 1.9\%$  under ISO and  $\alpha$ -chloralose, respectively ( $N = 5$ ). Similarly, frequency distribution and power of baseline CBF fluctuations were not significantly different (data not shown).

“Evoked” FP and CBF responses were dependent on the anesthetics used; the amplitude of evoked FP under ISO was

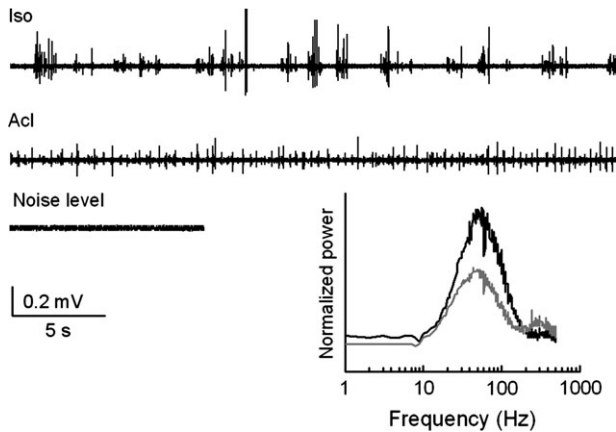


**Figure 2.** Baseline FP activity. The pattern of baseline FP activity differed depending on the anesthetics. Under ISO (Iso), burst-suppression pattern (i.e., depressed background activity alternating with high voltage activity) was typically observed, whereas  $\alpha$ -chloralose (Acl) caused frequent activity with small amplitude. Consequently, frequency composition of the baseline FP was different between ISO (black) and  $\alpha$ -chloralose (gray). The representative raw data of baseline FP were obtained from the same animal and compared with system noise level obtained after the animal was euthanized. The fast Fourier transform data was normalized by the noise level and averaged from all 5 animals.

slightly less than that under  $\alpha$ -chloralose (Fig. 3A), and evoked CBF under ISO was much less than under  $\alpha$ -chloralose (Fig. 3B). After each pulse of stimulation, baseline spontaneous activity under  $\alpha$ -chloralose was relatively suppressed unlike ISO (Fig. 3A). Our population data showed no significant differences in the mean amplitude of baseline FP between ISO and  $\alpha$ -chloralose (Fig. 3C), whereas the baseline CBF under ISO was  $45 \pm 8\%$  ( $N = 5$ ) higher than under  $\alpha$ -chloralose (Fig. 3D). ISO suppressed the evoked  $\Sigma$ FP by  $54 \pm 11\%$  (Fig. 3E) and evoked CBF peak by  $84 \pm 7\%$  (Fig. 3F) compared with  $\alpha$ -chloralose. These data clearly show that the stimulation parameters optimized for use with  $\alpha$ -chloralose are not effective for ISO-anesthetized rats. Note that variations across animals (SD/Mean) in evoked FP and CBF were slightly higher under  $\alpha$ -chloralose than ISO (Fig. 3E,F). Similarly, variations of heart rate and MABP (but not blood gases) across all 5 animals were observed to be higher under  $\alpha$ -chloralose than under ISO. This indicates that the larger variation across animals is due to unstable anesthetic states of  $\alpha$ -chloralose (Silverman and Muir 1993).

In our studies,  $\alpha$ -chloralose experiments followed ISO studies, which raises a concern as to whether the  $\alpha$ -chloralose experiments are affected by previously administered ISO. Due to ISO's fast recovery property ( $\sim 5$  min), its effect is negligible  $\sim 1$  h after its termination (ISO  $< \sim 0.1\%$ ). Thus, ISO is not likely to influence  $\alpha$ -chloralose studies. This notion is indirectly supported by 2 experimental evidences: 1) in our study, CBF response values ( $\sim 30$ – $50\%$ ) under  $\alpha$ -chloralose after ISO studies are in good agreement with reported values from previous  $\alpha$ -chloralose studies (i.e.,  $\sim 40\%$  peak response to standard stimulation; Silva and others 1999) and 2) evoked FP under ISO before and after  $\alpha$ -chloralose administration ( $n = 2$  animals) was found to be consistent (data not shown). These suggest that the  $\alpha$ -chloralose experiments are not affected by previously administered ISO in our study.

#### Evoked FP and CBF under ISO

To refine the stimulation parameters under ISO, one parameter (1.0 ms width, 1.0 mA current, or 125-ms interval [8 Hz

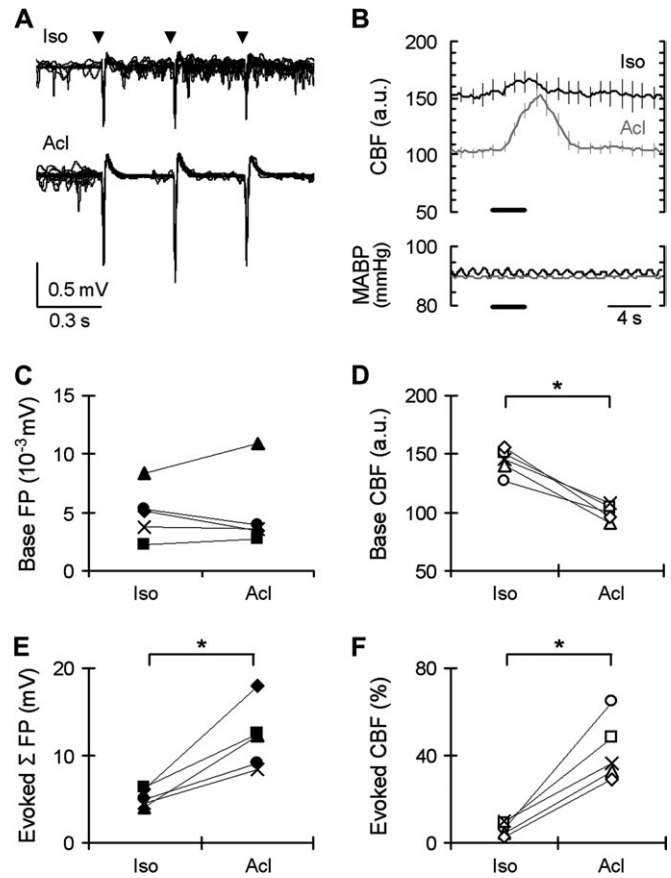


**Figure 3.** Evoked FP and CBF under  $\alpha$ -chloralose versus ISO. Evoked FP and CBF were compared under ISO (Iso) and  $\alpha$ -chloralose (Acl) in the same animal. The 10-pulse stimulation with 0.3 ms width, 1.2 mA current, and 333-ms interval was applied as previously shown under  $\alpha$ -chloralose (Silva and others 1999). (A) Typical FP traces including baseline activity (300 ms before stimulus onset) and initial 3 evoked responses (out of 10) to stimulation (arrowheads). Note that the poststimulus neural activity (i.e., after each stimulation pulse) was relatively active (noisy) under ISO but suppressed under  $\alpha$ -chloralose. The higher amplitude of evoked FP was evident in  $\alpha$ -chloralose compared with that in ISO. (B) Corresponding CBF responses under ISO (black) and  $\alpha$ -chloralose (gray) obtained from the same animal shown in panel (A). The evoked CBF was averaged across all 20 trials. Under ISO, the baseline CBF level was higher but evoked CBF was lower compared with  $\alpha$ -chloralose. Horizontal lines indicate the stimulation duration. Error bar indicates 1 SD for 20 trials. No observable changes in MABP during stimulation were confirmed. (C, D) Baseline FP (C) and baseline CBF (D) data from all 5 animals. Each symbol indicates the individual animal data. The baseline FP was not significantly different between ISO and  $\alpha$ -chloralose, whereas the baseline CBF was significantly higher under ISO than  $\alpha$ -chloralose. The baseline CBF under ISO was  $145 \pm 8\%$  of that under  $\alpha$ -chloralose.  $*P < 0.05$ . (E, F) Individual animal's data of  $\Sigma$ FP (E) and CBF peak response (F). The  $\Sigma$ FP and CBF peak were significantly higher in  $\alpha$ -chloralose ( $12 \pm 4$  mV and  $42 \pm 14\%$ ) than ISO ( $5 \pm 1$  mV and  $7 \pm 3\%$ ).

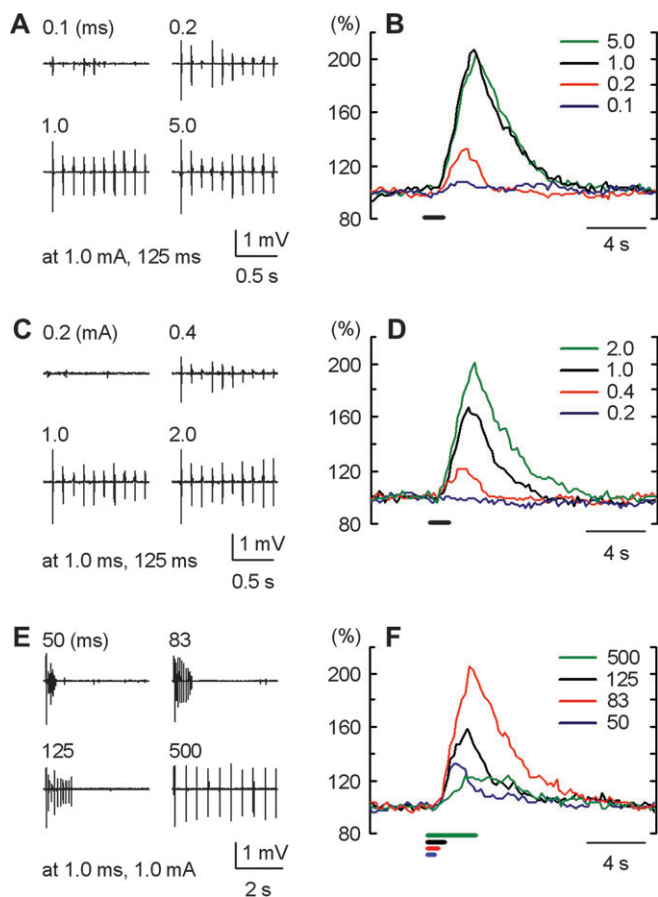
frequency]) was varied, whereas the other 2 parameters were fixed. These common parameters, 1.0 ms, 1.0 mA, and 125 ms, were determined based on our preliminary data that showed stable responses of both FP and CBF without influence on systemic blood pressure. Due to a limited experimental time, studies using all possible combinations of the 3 parameters were not performed.

Figure 4 shows FP traces (Fig. 4A,C,E) and the corresponding CBF time courses (Fig. 4B,D,F) in one representative animal. In order to show general trends, only 4 data points were selected in each condition out of 9, 10, and 9 for width (Fig. 4A,B), current (Fig. 4C,D), and interval variations (Fig. 4E,F), respectively. Similar trends were observed in all animals. In general, the

first evoked FP ( $FP_1$ ) was the largest among 10 consecutive evoked FPs. Remaining evoked FPs ( $FP_2$ - $FP_{10}$ ) were either attenuated or remained approximately constant. In particular, the interval variation (see Fig. 4E) profoundly affected the amplitude of  $FP_2$ - $FP_{10}$  despite the relatively constant  $FP_1$ ; a longer interval induced a higher amplitude of evoked  $FP_2$ - $FP_{10}$  (e.g.,  $0.3 \pm 0.2$  mV to  $0.11 \pm 0.03$  mV for 50 ms vs.  $1.7 \pm 1.0$  mV to  $1.3 \pm 0.9$  mV for 500-ms intervals,  $N = 7$ ). It should be noted that the time-to-onset of the evoked CBF was independent of the variation in stimulation parameters; its average value ranged from 0.4 to 0.6 s. On the other hand, time-to-peak and time-to-termination were dependent on stimulation parameters: both were extended with an increase in width (e.g., time-to-peak:  $2.2 \pm 0.3$  s for 0.1 ms vs.  $2.8 \pm 0.5$  s for 5 ms; time-to-termination:  $5.6 \pm 1.6$  s for 0.1 ms vs.  $9.9 \pm 1.5$  s for 5.0 ms;  $N = 5$ ), with an increase in current (e.g., time-to-peak:  $2.2 \pm 0.4$  s for

0.4 mA vs.  $2.9 \pm 0.3$  s for 2.0 mA; time-to-termination:  $5.0 \pm 1.6$  s for 0.4 mA vs.  $10.7 \pm 1.5$  s for 2.0 mA;  $N = 5$ ), and with an increase in interval (e.g., time-to-peak:  $1.9 \pm 0.3$  s for 50 ms vs.  $4.2 \pm 1.4$  s for 500 ms; time-to-termination:  $6.0 \pm 1.6$  s for 50 ms vs.  $10.4 \pm 1.8$  s for 500 ms;  $N = 7$ ).

To compare parameter-dependent FP and CBF responses across all animals,  $\sum FP$  and integral CBF in each study were normalized by the corresponding value induced by common stimulation with 1.0 ms width, 1.0 mA current, and 125-ms interval, respectively. Average normalized  $\sum FP$  and integral CBF of all animals were plotted as a function of width (Fig. 5A), current (Fig. 5B), and interval (Fig. 5C). Pulse width of 5.0 ms, current of 2.0 mA, and an interval of 500 ms induced the highest evoked  $\sum FP$  among respective parameter variation data. No significant differences in  $\sum FP$  were observed between widths of 5.0 versus  $\geq 0.5$  ms, currents of 2.0 versus  $\geq 1.4$  mA, and intervals of 500 versus  $\geq 250$  ms. On the other hand, the highest evoked



**Figure 4.** One animal's evoked FP and CBF data during variations of stimulation parameters under ISO. FP traces (A, C, and E) and corresponding CBF time courses (B, D, and F) induced by varied width (A, B), current (C, D), and onset-to-onset interval (E, F) in one representative animal were plotted. For each variation, only 4 data points (out of 9, 10, and 9 for width, current, and interval variations, respectively) were shown. The CBF response was normalized by the prestimulation baseline level. The horizontal lines in (B, D, and F) represent the stimulation durations. (A, B) Width (0.1, 0.2, 1.0, 5.0 ms) was varied with 1.0 mA current and 125-ms interval. The evoked FP and CBF similarly increased and reached a plateau with an increase in width. (C, D) Current (0.2, 0.4, 1.0, 2.0 mA) was varied with 1.0 ms width and 125-ms interval. The evoked FP and CBF monotonically increased with an increase in current. Note that 0.2 mA current was not enough to induce detectable FP and CBF changes. (E, F) Interval (50, 83, 125, 500 ms) was varied with 1.0 ms width and 1.0 mA current. Whereas the first evoked FP (out of 10) was relatively constant, the remaining evoked FPs (second to tenth) were preferentially affected by the intervals; a longer interval maintained a higher amplitude. In contrast, the highest peak CBF was observed at 83-ms interval.

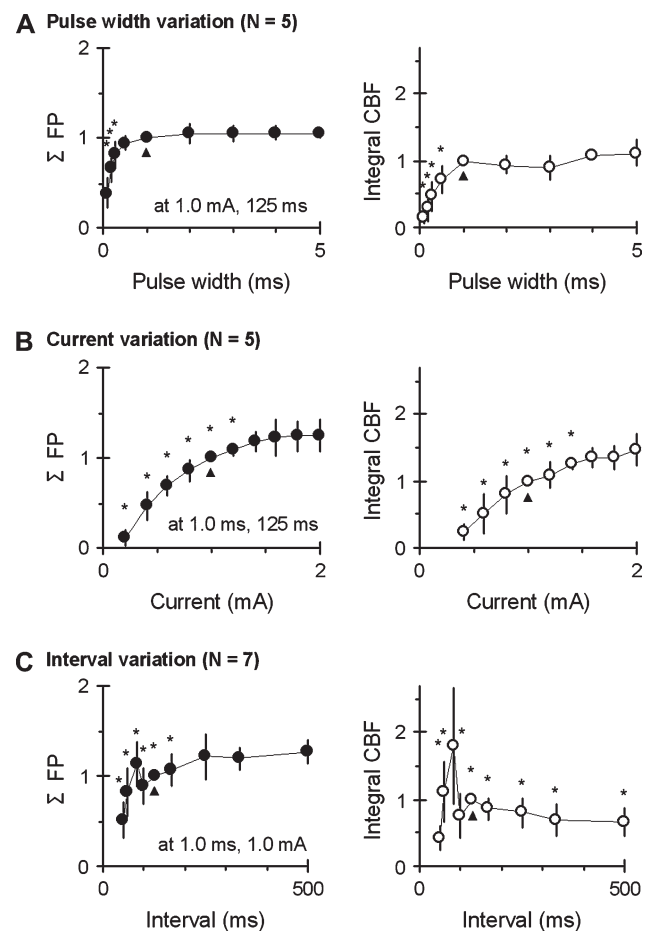


**Figure 5.** Parameter dependence of  $\sum FP$  and integral CBF. Normalized  $\sum FP$  (left) and integral CBF (right column) of all animals were plotted as a function of stimulation width (A) (with fixed current of 1.0 mA and interval of 125 ms,  $N = 5$ ), current (B) (with fixed width of 1.0 ms and interval of 125 ms,  $N = 5$ ), and interval (C) (with fixed width of 1.0 ms and current of 1.0 mA,  $N = 7$ ). The  $\sum FP$  and integral CBF were normalized by the values at the common stimulation (arrowhead; 1.0 ms width, 1.0 mA current, 125-ms interval) in each group. Note that the  $\sum FP$  and integral CBF reached a plateau for widths of 1.0–5.0 ms and for currents of 1.4–2.0 mA. For the interval variations, the  $\sum FP$  reached a plateau for interval of 250–500 ms, but the peak of integral CBF was consistently observed at the interval of 83 ms. Significant difference ( $*P < 0.05$ ) was shown by comparing the observed peak of  $\sum FP$  (5.0 ms width, 2.0 mA current, 500-ms interval) or peak of integral CBF (5.0 ms width, 2.0 mA current, 83-ms interval) within each variations groups. Error bar: 1 SD.

CBF was found for width of 5.0 ms, current of 2.0 mA, and an interval of 83 ms ( $80 \pm 26\%$ ,  $79 \pm 23\%$ , and  $73 \pm 32\%$  CBF peak, respectively). No significant differences in evoked CBF were found between widths of 5.0 versus  $\geq 1.0$  ms and currents of 2.0 versus  $\geq 1.6$  mA, whereas the evoked CBF response to 83-ms interval was significantly different from those at other intervals. Evoked FP and CBF responses to the maximized parameters (5.0 ms pulse, 2.0 mA current, and 83-ms interval) relative to the common parameters (1.0 ms pulse, 1.0 mA current, and 125-ms interval) were  $\sim 5\%$  and  $\sim 7\%$  higher in the width variation,  $\sim 25\%$  and  $\sim 17\%$  higher in the current variation, and  $\sim 14\%$  and  $\sim 38\%$  higher in the interval variation, respectively. Consequently, the combination of parameters 5.0 ms, 2.0 mA, and 83 ms could induce  $\sim 70\%$  higher evoked CBF than the common stimulation parameters, which induced a  $\sim 64\%$  CBF peak response. In fact, in our preliminary studies with 5.0 ms, 2.0 mA, and 83 ms parameters, the CBF response was 90–115%, which is similar to the expected CBF response (data not shown); however, one animal showed a change in MABP. Hence, to avoid unnecessary stress on the animals and potential global CBF changes caused by systemic blood pressure changes, the low end of the plateaued CBF response domain in pulse width (e.g., 1.0 ms) and current (e.g., 1.4–1.7 mA) was selected for BOLD fMRI experiments.

### BOLD fMRI under ISO

With refined stimulation parameters, the BOLD fMRI successfully detected a well-localized activation focus in the forepaw area of the primary somatosensory cortex contralateral to the stimulation side (Fig. 6A). No significant BOLD signal change in the ipsilateral somatosensory cortex was observed, which is consistent with the previously performed BOLD fMRI studies in rats under  $\alpha$ -chloralose (Lee and others 1999; Silva and others 1999).

The 12-Hz frequency with 10-pulse stimulation evoked the most significant and largest activation area compared with other frequencies (Fig. 6A). Similarly, the highest change in BOLD signal intensity was detected at 12-Hz frequency (Fig. 6B). This stimulation frequency dependence was consistently observed in all 5 animals. The significant difference in BOLD response was found for stimulation between 12 and 3 Hz and between 12 and 20 Hz (Fig. 6C). Overall, the frequency dependence of the BOLD signals agrees well with that of CBF measurement with LDF (Fig. 5C).

### Discussion

Three major issues were addressed in our studies. First, stimulation parameters optimized under  $\alpha$ -chloralose (Silva and others 1999) were not effective for ISO-anesthetized rats (Fig. 3), which was partly due to the lower evoked FP and/or higher baseline CBF under ISO anesthesia. Second, both evoked FP and CBF responses under ISO were improved when stimulation parameters were changed (Figs 4 and 5). Increasing the pulse width and current increased FP and CBF similarly, and then the response reached a plateau. However, the FP and CBF responses to the stimulation frequency (interval) were dissociated, indicating that the tuning of stimulation frequency is important for maximizing CBF response to a given number of stimulations. Finally, stimulation with refined parameters evoked robust, well-localized changes in BOLD fMRI signal in the somatosensory cortex for ISO-anesthetized rats (Fig. 6),

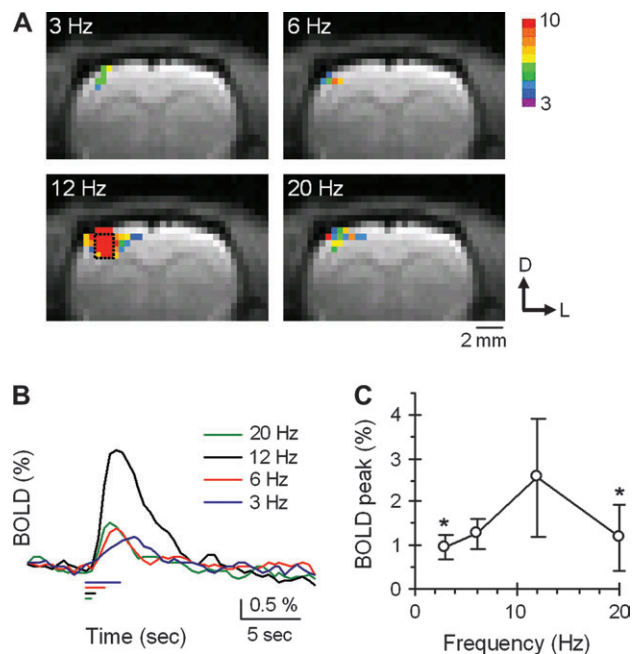


**Figure 6.** BOLD fMRI under ISO. (A) BOLD fMRI map obtained for various frequencies (3, 6, 12, 20 Hz) with refined parameters (1.0 ms width and 1.4 mA current) of 10-pulse stimulation in one representative animal. The color scale bar indicates  $t$ -values that were compared between baseline periods (10 images) and activation periods (4 images). The significant signal change was observed at the well-localized activity focus in contralateral forepaw area of the primary somatosensory cortex for all stimulation frequencies, but the robust activation area was obtained only for 12 Hz frequency ( $\sim 83$ -ms interval) stimulation. The rectangle in the image for 12-Hz stimulation indicates the position of  $3 \times 4$  pixels ROI. The same ROI was chosen for all stimulation conditions. D, dorsal; L, lateral. (B) Time courses of BOLD signal changes were calculated within the ROI shown in panel (A). The clear signal change was achieved at 12 Hz frequency. The horizontal bars show the stimulation duration corresponding to each stimulation frequency. (C) Population data on BOLD peak obtained from all 5 animals. Note that the 12-Hz frequency consistently evoked the highest BOLD signal change. Error bar: 1 SD.  $*P < 0.05$  (vs. 12-Hz stimulation).

which demonstrates that the ISO-anesthetized rodent model can be used for cerebrovascular activation studies. These findings highlight the necessity for complete data sets on neural activity, vascular response, and imaging signals to address hemodynamic-based functional imaging studies in anesthetized animals.

### Impact of Anesthetics on Neurovascular Responses

We observed that the amplitude of evoked FP was reduced by 54% under ISO compared with  $\alpha$ -chloralose using identical stimulation parameters (Fig. 3). This difference in evoked FP is clearly due to the different anesthetic actions on neural activity. ISO is believed to predominantly depress excitatory synaptic transmission (Larsen and Langmoen 1998; Richards 2002). For example, ISO inhibits excitatory transmitter release by reducing presynaptic excitability (Sandstrom 2004; Wu and others 2004) and enhances transmitter uptake in presynaptic terminals and astrocytes (Larsen and others 1997; Miyazaki and others 1997). The action of  $\alpha$ -chloralose involves potentiation of  $\gamma$ -aminobutyric acid (GABA) -induced currents via enhancement of GABA<sub>A</sub> receptor activity, generally known as the potent action site of general anesthetics (Kumamoto and Murata 1996; Garrett and Gan 1998). Because the hemodynamic signal is closely coupled to local neural activity, the reduced neural response observed under ISO (see Fig. 3E) can be a major cause of the

almost undetectable hemodynamic signal changes evoked by stimulation with the conventionally used parameters (e.g., 0.3 ms width, 1.0–1.5 mA current, and 3 Hz frequency).

Compared with  $\alpha$ -chloralose, the evoked FP under ISO was reduced by 54%, whereas the evoked CBF under ISO was reduced by 84%. This differential response indicates that hemodynamic coupling to neural activity is dependent on the anesthetic. This dissociation can be explained by the anesthetic-dependent changes in vascular reactivity. ISO has been known to cause vasodilation of cerebral arteries and intraparenchymal arterioles (Flynn and others 1992; Farber and others 1997), which may affect the vascular reactivity to local neural activation. It has also been consistently shown that ISO attenuates endothelium-dependent vasodilation (e.g., induced by acetylcholine) but not endothelium-independent vasodilation (e.g., induced by sodium nitroprusside) (Toda and others 1992; Uggeri and others 1992; Akata and others 1995). In addition, our study showed a 45% higher baseline CBF under ISO compared with  $\alpha$ -chloralose (Fig. 3D); these results generally agree with previously published CBF data (e.g., 70–90 mL/100 g/min under  $\alpha$ -chloralose (Ueki and others 1988; Lee and others 2001) versus 130–150 mL/100 g/min under 1 MAC ISO (Maekawa and others 1986; Lenz and others 1998). Differing baseline CBF significantly affects the magnitude of stimulation-induced hemodynamic responses (Cohen and others 2002); thus, the anesthetic-dependent baseline CBF may further contribute to the anesthetic-dependent couplings of hemodynamic response to neural activity (Shtoyerman and others 2000; Chen and others 2001). Further studies on the neural and/or vascular factors that mediate the intensity of hemodynamic response are needed to understand the hemodynamic coupling to neural activation.

#### **Optimization of Stimulation Parameters for Hemodynamic-Based Imaging**

We observed that evoked FP reached a plateau for the width and current variations during forepaw stimulation (Fig. 5A,B). This indicates that there is a threshold at which the maximum FP response is evoked; this threshold (>90% of peak) was observed at  $\geq 1.0$  ms width and  $\geq 1.4$  mA current. These parameter values were slightly higher than those reported under  $\alpha$ -chloralose in which threshold for FP response was  $\sim 0.3$  ms for width and  $\sim 1.0$  mA for current (Nielsen and Lauritzen 2001; Rosengarten and others 2003; Sheth and others 2004). Likewise, similar threshold levels were observed at  $\geq 1.0$  ms width and  $\geq 1.6$  mA current for CBF response under ISO (Fig. 5A,B). Activity-dependent augmentation and plateaued response of evoked CBF under ISO were similarly observed in functional hyperemia studies of width or current variations under  $\alpha$ -chloralose (Ngai and others 1995; Detre and others 1998; Silva and others 1999; Ances and others 2000; Nielsen and Lauritzen 2001; Nemoto and others 2004; Ureshi and others 2005).

In contrast, our results of the interval (frequency) variations indicate that there is an optimum frequency for maximizing the hemodynamic responses to given neural activity. Under 1 MAC ISO with 10-pulse stimulation, the optimum frequency that evoked the highest CBF and BOLD responses was achieved at  $\sim 12$  Hz ( $\sim 83$ -ms interval) (Figs 5C and 6C). Under  $\alpha$ -chloralose, the optimum frequency for the electrical forepaw or hind limb stimulation is within the range 1–5 Hz (Gyngell and others 1996; Detre and others 1998; Brinker and others 1999; Ngai and others 1999; Silva and others 1999; Matsuura and Kanno 2001;

Nielsen and Lauritzen 2001; Sheth and others 2004; Ureshi and others 2004). The peak of the hemodynamic response to frequency variations at 10 Hz under enflurane (Sheth and others 2003) is close to our result of 12 Hz, which possibly is due to the common actions of these halogenated ethers (enflurane vs. ISO) (Campagna and others 2003). It should be noted that a fixed stimulation time is commonly used, rather than a fixed number of pulses in the present study; for this case, further optimization of stimulation frequency may be needed.

Regarding the anesthetic-dependent neural activity, the observed difference in optimum frequency under ISO (enflurane) versus  $\alpha$ -chloralose can be related to the anesthetic-dependent refractory period of neural responses. It has been reported that the neural refractory period under  $\alpha$ -chloralose was 200–600 ms (Ogawa and others 2000; Ureshi and others 2004), whereas the excitatory postsynaptic current under ISO was observed with only  $\sim 20$  ms of interval with paired-pulse stimulation (Wu and others 2004). In our study, the difference in the poststimulus neural activity was observed; relatively silent under  $\alpha$ -chloralose but active (noisy) under ISO (Fig. 3A). In addition, our ISO experiment showed that the evoked FP was detected even for 20-Hz stimulation (Fig. 5C), supporting the idea that the neural refractory period differed depending on the anesthetics used.

In addition, we observed that evoked FP and CBF have a different frequency-dependence (Fig. 5C), which indicates that a nonlinear relationship exists in the neurovascular coupling. This mismatch between FP and CBF responses may be explained by the different transfer function from neural signals to vascular responses, depending on the stimulation frequency (Ureshi and others 2004). The frequency-dependent relationship between FP and CBF response is reported to be linear (Ngai and others 1999; Matsuura and Kanno 2001; Sheth and others 2003) and nonlinear (Nielsen and Lauritzen 2001; Sheth and others 2004), which may be explained by the different ranges of frequency variation (Hewson-Stoate and others 2005).

In the present study, the CBF response to 12 Hz frequency with 1.0 ms width and 1.0 mA current under ISO ( $\sim 70\%$  peak response) was observed to be 1.7 times higher than that at 3 Hz frequency with 0.3 ms width and 1.2 mA current under  $\alpha$ -chloralose ( $\sim 40\%$  peak response), whereas the  $\sum$ FP under ISO was only 1.1 times higher than under  $\alpha$ -chloralose. This further indicates that the transfer rate of neural response to hemodynamic signal depends on the anesthetics being used. These findings therefore indicate 2 major issues concerning the optimization of stimulation frequency in hemodynamic-based imaging: 1) the refractory period of neural responses (e.g.,  $\sum$ FP per a given time) and 2) the transfer rate of each neural activity to evoke hemodynamic signals (e.g., transfer function from  $\sum$ FP to vascular response).

#### **Hemodynamic-Based Functional Imaging in Anesthetized Animals**

$\alpha$ -Chloralose, a hypnotic agent, has been used because of its minimal depressant action on autonomic functions (Balis and Monroe 1964). However, an animal given  $\alpha$ -chloralose can only be used for terminal experiments (Silverman and Muir 1993). Further, dose-dependent or time-dependent variations have been observed in fMRI signals under  $\alpha$ -chloralose (Hyder and others 2002; Austin and others 2005). Because the analgesic or anesthetic qualities of  $\alpha$ -chloralose remain uncertain (Holzgrefe

and others 1987; Silverman and Muir 1993), the induction of  $\alpha$ -chloralose usually requires short-acting anesthetics (e.g., halothane or ISO) for preparation and is often administered as a cocktail with other injectable anesthetics (e.g., urethane or pentobarbital). These complex procedures and unstable states of anesthesia may be a source of the variations in fMRI with  $\alpha$ -chloralose (Sanganahalli and others 2005).

In contrast, the use of ISO offers 2 major advantages for functional studies. First, ISO has the stability of anesthetic depth coupled with the ease of simple noninvasive induction (Lukasik and Gillies 2003). This helps to maintain consistent animal conditions, unlike injectable anesthesia (especially bolus injection). Second, animals anesthetized with ISO recover quickly (Lukasik and Gillies 2003), which makes it possible to perform multiple noninvasive survival experiments over days and months in the same animal. It may even be feasible to allow the animal to breathe spontaneously during data collection (Fizanne and others 2003; Nemoto and others 2004), which makes possible the animal's use in noninvasive longitudinal studies. Therefore, fMRI studies using the stable and robust rodent ISO model can probe long-term changes in brain function in preclinical research (e.g., neurodegenerative diseases, such as stroke, Alzheimer's disease, and Parkinson's disease) as well as in basic neuroscience research (e.g., plasticity of the brain, such as development and learning).

## Conclusions

Neural and vascular responses are closely dependent on the anesthetics used. Therefore, optimizing stimulation parameters is necessary to maximize a hemodynamic response to a given neural activity. With the refined stimulation parameters, the ISO-anesthetized rodent model makes it possible to perform repeated survival fMRI studies in the same animal.

## Notes

We thank Iwao Kanno, Jeff Kershaw, Toshihiro Hayashi, Kristy Hendrich, and Michelle Tasker for helpful comments and discussions. This study was supported by the National Institutes of Health (EB003375 and NS044589). The 9.4-T system was funded in part by the NIH (RR17239). *Conflict of Interest:* None declared.

Address correspondence to Seong-Gi Kim, PhD, Department of Radiology, University of Pittsburgh, 3025 East Carson Street, Pittsburgh, PA 15203, USA. Email: kimg@pitt.edu.

## References

Akata T, Nakashima M, Kodama K, Boyle WA III, Takahashi S. 1995. Effects of volatile anesthetics on acetylcholine-induced relaxation in the rabbit mesenteric resistance artery. *Anesthesiology* 82:188-204.

Ances BM, Zarahn E, Greenberg JH, Detre JA. 2000. Coupling of neural activation to blood flow in the somatosensory cortex of rats is time-intensity separable, but not linear. *J Cereb Blood Flow Metab* 20:921-930.

Antognini JF, Wang XW, Carstens E. 1999. Quantitative and qualitative effects of isoflurane on movement occurring after noxious stimulation. *Anesthesiology* 91:1064-1071.

Arbit E, DiResta GR. 1996. Application of laser Doppler flowmetry in neurosurgery. *Neurosurg Clin N Am* 7:741-748.

Austin VC, Blamire AM, Allers KA, Sharp T, Styles P, Matthews PM, Sibson NR. 2005. Confounding effects of anesthesia on functional activation in rodent brain: a study of halothane and alpha-chloralose anesthesia. *Neuroimage* 24:92-100.

Balis GU, Monroe RR. 1964. The pharmacology of chloralose. A review. *Psychopharmacologia* 6:1-30.

Bonner R, Nossal R. 1981. Model for laser Doppler measurements of blood flow in tissue. *Appl Opt* 20:2097-2107.

Bonvento G, Charbonne R, Correze JL, Borredon J, Seylaz J, Lacombe P. 1994. Is alpha-chloralose plus halothane induction a suitable anesthetic regimen for cerebrovascular research? *Brain Res* 665:213-221.

Brinker G, Bock C, Busch E, Krep H, Hossmann KA, Hoehn-Berlage M. 1999. Simultaneous recording of evoked potentials and T2\*-weighted MR images during somatosensory stimulation of rat. *Magn Reson Med* 41:469-473.

Campagna JA, Miller KW, Forman SA. 2003. Mechanisms of actions of inhaled anesthetics. *N Engl J Med* 348:2110-2124.

Chen LM, Friedman RM, Ramsden BM, LaMotte RH, Roe AW. 2001. Fine-scale organization of SI (area 3b) in the squirrel monkey revealed with intrinsic optical imaging. *J Neurophysiol* 86:3011-3029.

Cohen ER, Ugurbil K, Kim SG. 2002. Effect of basal conditions on the magnitude and dynamics of the blood oxygenation level-dependent fMRI response. *J Cereb Blood Flow Metab* 22:1042-1053.

Detre JA, Ances BM, Takahashi K, Greenberg JH. 1998. Signal averaged laser Doppler measurements of activation-flow coupling in the rat forepaw somatosensory cortex. *Brain Res* 796:91-98.

Dirnagl U, Kaplan B, Jacewicz M, Pulsinelli W. 1989. Continuous measurement of cerebral cortical blood flow by laser-Doppler flowmetry in a rat stroke model. *J Cereb Blood Flow Metab* 9:589-596.

Duong TQ, Kim DS, Ugurbil K, Kim SG. 2001. Localized cerebral blood flow response at submillimeter columnar resolution. *Proc Natl Acad Sci USA* 98:10904-10909.

Eger EI 2nd, Saidman LJ, Brandstater B. 1965. Minimum alveolar anesthetic concentration: a standard of anesthetic potency. *Anesthesiology* 26:756-763.

Farber NE, Harkin CP, Niedfeldt J, Hudetz AG, Kampine JP, Schmeling WT. 1997. Region-specific and agent-specific dilation of intracerebral microvessels by volatile anesthetics in rat brain slices. *Anesthesiology* 87:1191-1198.

Fizanne L, Fromy B, Preckel MP, Sigaucho-Roussel D, Saumet JL. 2003. Effect of isoflurane on skin-pressure-induced vasodilation. *J Vasc Res* 40:416-422.

Flynn NM, Buljubasic N, Bosnjak ZJ, Kampine JP. 1992. Isoflurane produces endothelium-independent relaxation in canine middle cerebral arteries. *Anesthesiology* 76:461-467.

Garrett KM, Gan J. 1998. Enhancement of gamma-aminobutyric acidA receptor activity by alpha-chloralose. *J Pharmacol Exp Ther* 285:680-686.

Gyngell ML, Bock C, Schmitz B, Hoehn-Berlage M, Hossmann KA. 1996. Variation of functional MRI signal in response to frequency of somatosensory stimulation in alpha-chloralose anesthetized rats. *Magn Reson Med* 36:13-15.

Hall RD, Lindholm EP. 1974. Organization of motor and somatosensory neocortex in the albino rat. *Brain Res* 66:23-38.

Hayton SM, Kriss A, Muller DP. 1999. Comparison of the effects of four anaesthetic agents on somatosensory evoked potentials in the rat. *Lab Anim* 33:243-251.

Hewson-Stoate N, Jones M, Martindale J, Berwick J, Mayhew J. 2005. Further nonlinearities in neurovascular coupling in rodent barrel cortex. *Neuroimage* 24:565-574.

Holzgreffe HH, Everitt JM, Wright EM. 1987. Alpha-chloralose as a canine anesthetic. *Lab Anim Sci* 37:587-595.

Hyder F, Behar KL, Martin MA, Blamire AM, Shulman RG. 1994. Dynamic magnetic resonance imaging of the rat brain during forepaw stimulation. *J Cereb Blood Flow Metab* 14:649-655.

Hyder F, Rothman DL, Shulman RG. 2002. Total neuroenergetics support localized brain activity: implications for the interpretation of fMRI. *Proc Natl Acad Sci USA* 99:10771-10776.

Kim DS, Duong TQ, Kim SG. 2000. High-resolution mapping of iso-orientation columns by fMRI. *Nat Neurosci* 3:164-169.

Kumamoto E, Murata Y. 1996. Enhancement by lanthanide of general anesthetic-induced GABAA-receptor current in rat septal cholinergic neurons in culture. *J Neurophysiol* 75:2294-2299.

Larsen M, Hegstad E, Berg-Johnsen J, Langmoen IA. 1997. Isoflurane increases the uptake of glutamate in synaptosomes from rat cerebral cortex. *Br J Anaesth* 78:55-59.

- Larsen M, Langmoen IA. 1998. The effect of volatile anaesthetics on synaptic release and uptake of glutamate. *Toxicol Lett* 100:101-59-64.
- Lee SP, Duong TQ, Yang G, Iadecola C, Kim SG. 2001. Relative changes of cerebral arterial and venous blood volumes during increased cerebral blood flow: implications for BOLD fMRI. *Magn Reson Med* 45:791-800.
- Lee SP, Silva AC, Ugurbil K, Kim SG. 1999. Diffusion-weighted spin-echo fMRI at 9.4 T: microvascular/tissue contribution to BOLD signal changes. *Magn Reson Med* 42:919-928.
- Lees P. 1972. Pharmacology and toxicology of alpha chloralose: a review. *Vet Rec* 91:330-333.
- Lenz C, Frietsch T, Futterer C, Rebel A, van Ackern K, Kuschinsky W, Waschke KF. 1999. Local coupling of cerebral blood flow to cerebral glucose metabolism during inhalational anesthesia in rats: desflurane versus isoflurane. *Anesthesiology* 91:1720-1723.
- Lindauer U, Villringer A, Dirnagl U. 1993. Characterization of CBF response to somatosensory stimulation: model and influence of anesthetics. *Am J Physiol* 264:H1223-H1228.
- Liu ZM, Schmidt KF, Sicard KM, Duong TQ. 2004. Imaging oxygen consumption in forepaw somatosensory stimulation in rats under isoflurane anesthesia. *Magn Reson Med* 52:277-285.
- Logothetis NK, Guggenberger H, Peled S, Pauls J. 1999. Functional imaging of the monkey brain. *Nat Neurosci* 2:555-562.
- Lukasik VM, Gillies RJ. 2003. Animal anaesthesia for in vivo magnetic resonance. *NMR Biomed* 16:459-467.
- Maekawa T, Tommasino C, Shapiro HM, Keifer-Goodman J, Kohlenberger RW. 1986. Local cerebral blood flow and glucose utilization during isoflurane anesthesia in the rat. *Anesthesiology* 65:144-151.
- Mandeville JB, Marota JJ, Kosofsky BE, Keltner JR, Weissleder R, Rosen BR, Weisskoff RM. 1998. Dynamic functional imaging of relative cerebral blood volume during rat forepaw stimulation. *Magn Reson Med* 39:615-624.
- Matsuura T, Kanno I. 2001. Quantitative and temporal relationship between local cerebral blood flow and neuronal activation induced by somatosensory stimulation in rats. *Neurosci Res* 40:281-290.
- Miyazaki H, Nakamura Y, Arai T, Kataoka K. 1997. Increase of glutamate uptake in astrocytes: a possible mechanism of action of volatile anesthetics. *Anesthesiology* 86:1359-1366.
- Moon C, Fukuda M, Kim SG. 2004. Analysis of continuous intrinsic optical imaging data. Program No. 920.13, 2004 Abstract Viewer/Itinerary Planner. Washington, DC: Society for Neuroscience.
- Narayan SM, Santori EM, Toga AW. 1994. Mapping functional activity in rodent cortex using optical intrinsic signals. *Cereb Cortex* 4:195-204.
- Nemoto M, Sheth S, Guiou M, Pouratian N, Chen JW, Toga AW. 2004. Functional signal- and paradigm-dependent linear relationships between synaptic activity and hemodynamic responses in rat somatosensory cortex. *J Neurosci* 24:3850-3861.
- Ngai AC, Jolley MA, D'Ambrosio R, Meno JR, Winn HR. 1999. Frequency-dependent changes in cerebral blood flow and evoked potentials during somatosensory stimulation in the rat. *Brain Res* 837:221-228.
- Ngai AC, Meno JR, Winn HR. 1995. Simultaneous measurements of pial arteriolar diameter and laser-Doppler flow during somatosensory stimulation. *J Cereb Blood Flow Metab* 15:124-127.
- Nielsen AN, Lauritzen M. 2001. Coupling and uncoupling of activity-dependent increases of neuronal activity and blood flow in rat somatosensory cortex. *J Physiol* 533:773-785.
- Ogawa S, Lee TM, Stepnoski R, Chen W, Zhu XH, Ugurbil K. 2000. An approach to probe some neural systems interaction by functional MRI at neural time scale down to milliseconds. *Proc Natl Acad Sci USA* 97:11026-11031.
- Paxinos G, Watson C. 1986. The rat brain in stereotaxic coordinates. California: Academic Press.
- Richards CD. 2002. Anaesthetic modulation of synaptic transmission in the mammalian CNS. *Br J Anaesth* 89:79-90.
- Rosengarten B, Lutz H, Hossmann KA. 2003. A control system approach for evaluating somatosensory activation by laser-Doppler flowmetry in the rat cortex. *J Neurosci Methods* 130:75-81.
- Sandstrom DJ. 2004. Isoflurane depresses glutamate release by reducing neuronal excitability at the Drosophila neuromuscular junction. *J Physiol* 558:489-502.
- Sanganahalli BG, Herman P, Hyder F. 2005. Influence of volatile induction agents on fMRI and neural activity. *J Cereb Blood Flow Metab* 25:s395.
- Sheth S, Nemoto M, Guiou M, Walker M, Pouratian N, Toga AW. 2003. Evaluation of coupling between optical intrinsic signals and neuronal activity in rat somatosensory cortex. *Neuroimage* 19:884-894.
- Sheth SA, Nemoto M, Guiou M, Walker M, Pouratian N, Toga AW. 2004. Linear and nonlinear relationships between neuronal activity, oxygen metabolism, and hemodynamic responses. *Neuron* 42:347-355.
- Shtoyerman E, Arieli A, Slovov H, Vanzetta I, Grinvald A. 2000. Long-term optical imaging and spectroscopy reveal mechanisms underlying the intrinsic signal and stability of cortical maps in V1 of behaving monkeys. *J Neurosci* 20:8111-8121.
- Silva AC, Lee SP, Yang G, Iadecola C, Kim SG. 1999. Simultaneous blood oxygenation level-dependent and cerebral blood flow functional magnetic resonance imaging during forepaw stimulation in the rat. *J Cereb Blood Flow Metab* 19:871-879.
- Silverman J, Muir WW III. 1993. A review of laboratory animal anesthesia with chloral hydrate and chloralose. *Lab Anim Sci* 43:210-216.
- Stern MD, Lappe DL, Bowen PD, Chimosky JE, Holloway GA Jr, Keiser HR, Bowman RL. 1977. Continuous measurement of tissue blood flow by laser-Doppler spectroscopy. *Am J Physiol* 232:H441-H448.
- Toda H, Nakamura K, Hatano Y, Nishiwada M, Kakuyama M, Mori K. 1992. Halothane and isoflurane inhibit endothelium-dependent relaxation elicited by acetylcholine. *Anesth Analg* 75:198-203.
- Ueki M, Linn F, Hossmann KA. 1988. Functional activation of cerebral blood flow and metabolism before and after global ischemia of rat brain. *J Cereb Blood Flow Metab* 8:486-494.
- Ueki M, Mies G, Hossmann KA. 1992. Effect of alpha-chloralose, halothane, pentobarbital and nitrous oxide anesthesia on metabolic coupling in somatosensory cortex of rat. *Acta Anaesthesiol Scand* 36:318-322.
- Uggeri MJ, Proctor GJ, Johns RA. 1992. Halothane, enflurane, and isoflurane attenuate both receptor- and non-receptor-mediated EDRF production in rat thoracic aorta. *Anesthesiology* 76:1012-1017.
- Ureshi M, Kershaw J, Kanno I. 2005. Nonlinear correlation between field potential and local cerebral blood flow in rat somatosensory cortex evoked by changing the stimulus current. *Neurosci Res* 51:139-145.
- Ureshi M, Matsuura T, Kanno I. 2004. Stimulus frequency dependence of the linear relationship between local cerebral blood flow and field potential evoked by activation of rat somatosensory cortex. *Neurosci Res* 48:147-153.
- van Bruggen N, Busch E, Palmer JT, Williams SP, de Crespigny AJ. 1998. High-resolution functional magnetic resonance imaging of the rat brain: mapping changes in cerebral blood volume using iron oxide contrast media. *J Cereb Blood Flow Metab* 18:1178-1183.
- Wu XS, Sun JY, Evers AS, Crowder M, Wu LG. 2004. Isoflurane inhibits transmitter release and the presynaptic action potential. *Anesthesiology* 100:663-670.